

## Journal Pre-proofs

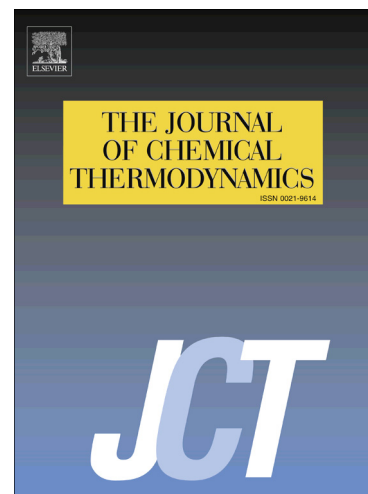
Experimental examination and thermodynamic description of the ternary Bi-Ge-Ga,Zn systems

Aleksandar Djordjevic, Milena Premovic, Dusko Minic, Vladan Cosovic,  
Dragan Manasijevic

PII: S0021-9614(19)30582-8  
DOI: <https://doi.org/10.1016/j.jct.2019.106000>  
Reference: YJCHT 106000

To appear in: *J. Chem. Thermodynamics*

Received Date: 20 June 2019  
Revised Date: 1 October 2019  
Accepted Date: 27 October 2019



Please cite this article as: A. Djordjevic, M. Premovic, D. Minic, V. Cosovic, D. Manasijevic, Experimental examination and thermodynamic description of the ternary Bi-Ge-Ga,Zn systems, *J. Chem. Thermodynamics* (2019), doi: <https://doi.org/10.1016/j.jct.2019.106000>

This is a PDF file of an article that has undergone enhancements after acceptance, such as the addition of a cover page and metadata, and formatting for readability, but it is not yet the definitive version of record. This version will undergo additional copyediting, typesetting and review before it is published in its final form, but we are providing this version to give early visibility of the article. Please note that, during the production process, errors may be discovered which could affect the content, and all legal disclaimers that apply to the journal pertain.

## Experimental examination and thermodynamic description of the ternary Bi-Ge-Ga,Zn systems

Aleksandar Djordjevic<sup>1</sup>, Milena Premovic<sup>1,\*</sup>, Dusko Minic<sup>1</sup>, Vladan Cosovic<sup>2</sup> and Dragan Manasijevic<sup>3</sup>

<sup>1</sup> University of Priština, Faculty of Technical Science, Kneza Milosa 7,  
40000 Kos. Mitrovica, Serbia

<sup>2</sup> University of Belgrade, Institute of Chemistry, Technology and Metallurgy, Belgrade, Serbia

<sup>3</sup> University of Belgrade, Technical Faculty in Bor, VJ 12, 19210 Bor, Serbia

## Abstract:

Due to the wide application of systems based on germanium ternary Bi-Ga-Ge and Bi-Ge-Zn systems were experimentally tested in this study. Used experimental techniques were scanning electron microscope with energy dispersive spectroscopy (SEM-EDS), x-ray diffraction (XRD) and differential thermal analysis (DTA). Three groups of samples were prepared and tested. Alloys were from two isothermal sections at 100 and 300 °C and three vertical sections. Obtained results of experimental tests were compared with predicted phase diagrams. Comparison of EDS and DTA results with calculated phase diagrams of the ternary Bi-Ga-Ge system results in good agreement. While for Bi-Ge-Zn was necessary to introduce new ternary parameters. Introduced ternary parameters were based on experimental results from this study. The thermodynamic descriptions of the ternary Bi-Ga-Ge and Bi-Ge-Zn systems have been developed by using CALPHAD method. Reasonable agreement between experimental data and the calculated phase diagrams has been reached for both ternary Bi-Ga-Ge and Bi-Ge-Zn

systems. The liquid projection and invariant equilibria have been calculated by using obtained thermodynamic parameters.

Keywords: phase diagram, Bi-Ga-Ge, Bi-Ge-Zn, liquidus projection.

Corresponding author: [milena.premovic@gmail.com](mailto:milena.premovic@gmail.com) (Milena Premovic)

## 1. Introduction

Germanium and germanium based alloys are being investigated because they are used widely as a phase change memory materials (PCM materials) [1-3]. Binary alloy Ge<sub>15</sub>Sb<sub>85</sub> [4] and ternary alloys such as Ge<sub>1</sub>Sb<sub>4</sub>Te<sub>7</sub>, Ge<sub>1</sub>Sb<sub>2</sub>Te<sub>4</sub>, Ge<sub>2</sub>Sb<sub>2</sub>Te<sub>5</sub>, and Ge<sub>3</sub>Sb<sub>2</sub>Te<sub>6</sub> [5] were selected as potential phase-change materials. The ternary alloy Ge<sub>2</sub>Sb<sub>2</sub>Te<sub>5</sub> was shown to be most favorable and this alloy appears to be suitable for use in memory devices. On the other hand germanium based alloys are widely used in industry, for making different electronic and optoelectronic devices [6,7], transistors, semiconductors, integrated circuits, etc. [8-11]. Germanium is also important semiconductors, and the studies of phase relations in the semiconducting alloy systems are essential for the development of new and the improvement of existing semiconductor materials [12]. It is known that the addition of Bi to Ge-based materials can significantly alter their semiconducting properties and also lead to a development of entirely new types of semiconducting materials [13]. In that sense, the knowledge of phase equilibria represents a valuable tool. Due to the limited number of research related to multicomponent germanium systems, it is necessary to test more systems based on germanium. Selected systems in this study are based on Bi-Ge system since up to now there is limited number of studies of ternary systems based on Bi-Ge-X (X=In,Sn,Sb,Si,Ag) alloys [14-17].

In this work two ternary Bi-Ga-Ge and Bi-Ge-Zn systems were studied. Studied ternary alloys were from isothermal section at 100 °C and 300 °C and three vertical sections for both ternary systems. Experimental techniques were differential thermal analysis (DTA), scanning electron microscopy (SEM) with energy dispersive spectrometry (EDS) and X-ray powder diffraction (XRD). Experimentally determined results were used for thermodynamic modelling of the ternary system.

Experimental results for alloys from ternary Bi-Ga-Ge were compared with calculated phase diagrams of isothermal section at 100 °C and 300 °C and vertical sections and reasonable agreement between calculated phase diagrams and experimental data was obtained.

In the ternary Bi-Ge-Zn it was necessary to introduce new ternary parameters for the liquid phase. By adding new ternary parameters good agreement between calculated phase diagrams and experimental results has been reached.

## 2. Experimental procedure

All ternary samples with total masses of about 3 g were prepared from elements high purity (99.999 at. %) Bi, Ge, Ga and Zn produced by Alfa Aesar (Germany) in an induction furnace under high-purity argon atmosphere (Table 1). The average weight loss of the samples during induction melting was about 0.5 mass %.

Table 1. Sample table with the purities provided by the supplier and the samples are used as received.

Samples were subjected for the SEM-EDS and XRD investigation were put into quartz glass ampoules, sealed under vacuum and annealed at 100 °C for four weeks, and another group of samples was annealed at 300 °C for four weeks. Upon annealing, the samples were immediately quenched into ice water so as to retain the equilibrium compositions at designated temperatures.

The compositions of samples and coexisting phases were determined using JEOL JSM-6460 scanning electron microscope with energy dispersive spectroscopy (EDS) (Oxford Instruments X-act). EDS has been calibrated with the external standard with registration number 7774 and 7775, produced by Micro Analysis Consultants Ltd., Cambridge, UK. Determination of overall compositions of annealed samples was done by analyzing as large as possible surface of the samples. The compositions of co-existing phases were determined by examining the surface of the same phase at a different parts of the sample (at least five different positions of the same phase are examined per phase).

Powder XRD data for phase identification of samples were recorded on a D2 PHASER (Bruker, Karlsruhe, Germany) powder diffractometer equipped with a dynamic scintillation detector and ceramic X-ray Cu tube (KFL-Cu-2K) in a  $2\theta$  range from 10° to 75° with a step size of 0.02°. The patterns were analyzed using the Topas 4.2 software, ICDD databases PDF2 (2013). The instrument was calibrated with Bruker standard, Korundprobe A26-B26-S, beside this standard, ten different powder elements (high purity elements bought from Alfa Aesar) were used as a standard in process of calibration.

Phase transition temperatures were determined by DTA method by using DTG-60A series from Shimadzu. Device were calibrated with high purity elements produced by Alfa Aesar (Al, Ag, Bi, Ga, Ge, Sn, Sb, Zn, Ni). Alumina crucibles were used and measurements were performed under flowing argon atmosphere. The samples were placed in alumina crucibles and characteristic

temperatures were recorded under protective flowing Ar atmosphere (produced by MESSER) during heating rate of 5 °C/min. Weights of the analyzed alloy samples were between 30 and 40 mg and a reference material was an empty alumina crucible. Determination of phase transition temperatures from DTA results was carried out according to recommendations from the literature [18,19]. The liquidus and temperatures of monovariant phase transitions were determined from peak maxima while the solidus temperatures and the temperatures of invariant reactions were determined from onset temperatures of the corresponding peaks.

### 3. Thermodynamic calculation of binary systems

Ternary Bi-Ga-Ge and Bi-Ge-Zn systems has not been experimentally investigated and thermodynamically assessed up to now. However, constitutive binary Bi-Ga, Bi-Ge, Ga-Ge, Bi-Zn and Ge-Zn systems were extensively studied in the past and reliable thermodynamic datasets for these binary systems are available in the literature [20-24]. Optimized thermodynamic parameters of these binary systems are from different source (binary Bi-Ge Chevalier [20], binary Bi-Ga Girard [21], binary Ga-Ge Olesinski and Abbaschian [22], binary Bi-Zn Malakhov [23] and binary Ge-Zn Chevalier [24]) and calculated binary phase diagrams are given in Figure 1.

Figure 1. Calculated binary phase diagrams a) Bi-Ge system [20], b) Bi-Ga system [21], c) Ga-Ge system [22], d) Bi-Zn system [23] and e) Ge-Zn system [24].

Based on the literature information for binary sub-systems crystallographic data [25-28] for solid phases are summarized in Table 2.

Table 2. Considered phase, their crystallographic data and database names for the phases of the ternary Bi-Ga-Ge and Bi-Ge-Zn systems.

Based on the phase equilibria and crystallographic data for the constitutive binary systems in the ternary Bi-Ga-Ge system should appear liquid phase and three solid solutions (Bi), (Ga) and (Ge), and in ternary Bi-Ge-Zn system should appear liquid phase and three solid solutions (Bi), (Ge) and (Zn). Since ternary system is not investigated before there is no information about ternary compounds.

#### 4. Experimental results

##### 4.1. Ternary Bi-Ga-Ge system

Twelve ternary samples are tested with DTA method. Tested samples are from three vertical sections Bi-GaGe, Ga-BiGe and Ge-BiGa. Temperatures of phase transformations are taken from peaks according to the literature recommendations [18,19]. Results of the tests are summarized in Table 3.

Table 3. Phase transition temperatures of the studied alloys from the ternary Bi-Ga-Ge system determined by DTA at pressure  $p=0.1$  MPa<sup>a</sup>.

On ten samples are detected three peaks, while on two samples four peaks are detected. It can be notice that first detected peak of each sample have similar value of temperatures and it can be assumed that detected temperatures are related to the same transformation. Second detected

temperature is ternary transition reaction while last detected temperature on all samples is liquidus temperature. Experimental temperatures are compared with calculated vertical sections (Figure 2).

Figure 2. Calculated vertical sections of the ternary Bi-Ga-Ge system compared with DTA experimental results: a) Bi-GaGe, b) Ge-BiGa and c) Ga-BiGe.

From figure 2, can be notice good agreement with calculation and experimental results. From calculation it is clear that first detected temperature of all samples is related to the same transformation  $L \rightarrow (\text{Bi}) + (\text{Ga}) + (\text{Ge})$ . By calculation temperature of ternary reaction  $L \rightarrow (\text{Bi}) + (\text{Ga}) + (\text{Ge})$  is 29.57 °C and by experiment temperature is in range from 32.9 to the 37.6 °C.

As a next step five ternary samples annealed at 100 °C, were tested by using SEM-EDS and XRD method. Results of tests are summarized in Table 4.

Table 4. Combined results of SEM-EDS and XRD analyzes of the selected Bi-Ga-Ge alloys annealed at  $T=100$  °C (standard uncertainty (u):  $u(T)=1.0$  °C) at pressure  $p=0.1$  MPa (standard uncertainty (u):  $u(p)=1$  kPa).

According to the EDS and XRD results in all tested samples three same phases are detected. Detected phases are (Bi), (Ge) and L. EDS results shows that (Bi) solid solution is rich with bismuth and dissolves neglected amount of other two elements, (Ge) solid solution is rich with germanium and dissolves neglected amount of other two elements, and liquid phase dissolves



neglected amount bismuth and germanium. Microstructure of sample 2 annealed at 100 °C are presented in Figure 3.

Figure 3. SEM micrographs of sample 2.

On given microstructures are marked detected phases by EDS and XRD tests. In presented microstructure (Ge) solid solution appears as a dark phase, (Bi) solid solution as a gray phase and liquid phase as a light phase.

Since samples were annealed at 100 °C, EDS composition of phases are compared with calculated isothermal section at 100 °C. Figure 4, present comparison of EDS results from Table 4 and calculated isothermal section at 100 °C. EDS results on figure are marked with same symbol but in different color. Different color is in order to distinguish EDS composition of different samples.

Figure 4. Calculated isothermal section at 100 °C compared with EDS results given in Table 4.

Calculated isothermal section have three phase regions, two are two-phase regions (Bi)+L and (Ge)+L, and one is three-phase region (Ge)+L+(Bi). All experimentally tested samples are located in three-phase region (Ge)+L+(Bi) same phase region as experimentally detected. Experimental compositions of phases are in agreement with calculated compositions.

As a next step, five ternary samples annealed at 300 °C were tested with EDS and XRD. Results of those tests are summarized in Table 5.

Table 5. Combined results of SEM-EDS and XRD analyzes of the selected Bi-Ga-Ge alloys annealed at  $T=300$  °C (standard uncertainty (u):  $u(T)=1.0$  °C) at pressure  $p=0.1$  MPa (standard uncertainty (u):  $u(p)=1$  kPa).

As it is given in Table 5, in all tested samples same two phases are detected. Detected phases are L and (Ge) solid solution. From EDS results it is detected that (Ge) solid solution is rich with germanium and can dissolve neglected amount of gallium and bismuth. EDS result shows that L phase have different composition depending on composition of the samples. So samples rich with bismuth result to have L, phase rich with bismuth.

As an illustration one SEM microstructure of tested sample 4 is given in Figure 5.

Figure 5. SEM micrographs of sample 4.

From microstructure it is visible that (Ge) solid solution appears as a gray phase and L phase a light phase.

Since tested samples are annealed at 300 °C, EDS results of tested samples are compared with calculated isothermal section at 300 °C. Figure 6, presents calculated isothermal section at 300 °C compared with EDS results.

Figure 6. Calculated isothermal section at 300 °C compared with EDS results given in Table 5.

Calculated isothermal section at 300 °C consists of two phase regions. One is single phase region and other is two-phase region L+(Ge). By comparing EDS composition of the tested samples it is located that all samples are from two-phase region L+(Ge) same phases as experimentally

detected. EDS compositions of the phases are in good agreement with calculated compositions of the phases.

Based on presented results it is not necessary to introduce new parameters for description of the ternary Bi-Ga-Ge system. So used thermodynamic data set have been used for calculation of liquidus projection and invariant reactions.

Figure 7, presents prediction of liquidus projection of the ternary Bi-Ga-Ge system with the enlarged Bi-Ga rich region.

Figure 7. Liquidus projection of the ternary Bi-Ga-Ge system with the enlarged Bi-Ga rich region.

Four fields of primary crystallization (L, (Ga), (Bi) and (Ge)) are visible on predicted liquidus projection. Two invariant reactions were predicted of which one is ternary eutectic reaction and other is ternary transition reaction. Details of reactions are listed in Table 6.

Table 6. Predicted invariant reaction of the ternary Bi-Ga-Ge system.

Calculated ternary eutectic reaction is experimentally detected with 12 samples tested by DTA (see Table 3), and determined temperature of reaction is close to the calculated one.

#### 4.2. Ternary Bi-Ge-Zn system

Twelve ternary samples were analyzed by using DTA. Chosen samples were from three different vertical sections with four samples per vertical section. Determination of phase transition temperatures from DTA results was carried out according to recommendations from the literature [18,19]. The results of DTA studies are summarized in Table 7.

Table 7. Phase transition temperatures of the studied alloys from the ternary

Bi-Ge-Zn system determined by DTA at pressure  $p=0.1$  MPa<sup>a</sup>.

From DTA results given in Table 7, it is detected that first detected temperature in all samples belongs to the same phase transformation. Detected temperature in all samples is close one to another and is in range from 246.1 to the 261.8 °C. Last temperature detected on DTA curve belongs to the liquidus transformation and in the samples from vertical section Ge-BiZn it is noticed trend that with the increase of germanium content in samples temperature increase respectively. In samples from vertical sections Zn-BiGe it is noticed trend of decrease in temperature with increasements of the Zn content in samples, respectively.

In next step, five samples annealed at 100 °C for four weeks, were tested with SEM-EDS and XRD. Obtained results with those two techniques are presented in Table 8.

Table 8. Combined results of SEM-EDS and XRD analyzes of the selected Bi-Ge-Zn alloys annealed at  $T=100$  °C (standard uncertainty (u):  $u(T)=1.0$  °C) at pressure  $p=0.1$  MPa (standard uncertainty (u):  $u(p)=1$  kPa).

In all five tested samples same three phases were detected. In all samples detected phases are (Ge), (Bi) and (Zn) solid solutions. Compositions of the detected phases in all samples are close one to another. Detected (Ge) solid solution in all samples is rich with germanium and can dissolve neglected amount of bismuth and zinc. Solid solution (Bi), is rich with bismuth. Third

detected is (Zn) solid solution rich with zinc with range of Zn from 98.63 to the 99.50 at. %, and neglected solubility of Bi and Ge.

Since in all tested samples same phases are detected, one SEM microstructure of sample 2 is presented in Fig. 8, with marked name of phases.

Figure 8. SEM micrograph of sample 2.

Figure 8 presents microstructure of sample 2 on which are marked three experimentally detected phases. (Ge) solid solution is dark phase, (Zn) phase as a gray phase and (Bi) phase as a light gray phase.

Five samples annealed at 300 °C were tested with SEM-EDS and XRD. Results of tests are given in Table 9.

Table 9. Combined results of SEM-EDS and XRD analyzes of the selected Bi-Ge-Zn alloys annealed at  $T=300$  °C (standard uncertainty (u):  $u(T)=1.0$  °C) at pressure  $p=0.1$  MPa (standard uncertainty (u):  $u(p)=1$  kPa).

With five tested samples two different phase regions were detected. Samples 1, 2 and 3 detected three phases. Detected three-phase region is  $L+(Ge)+(Zn)$ , solid solution (Ge) is rich with germanium and (Zn) solid solution with zinc, and both are dissolve neglected amount of other two elements. Detected L phase in all three samples is rich with bismuth in range from 86.29 to

the 87.39 at. % and residual are zinc and germanium. In samples 4 and 5, two same phases are detected, L and (Ge) solid solution.

SEM microstructure of sample 4 is presented in Figure 9 as one illustration.

Figure 9. SEM micrograph of sample 4.

Micrograph of sample 4, given on Fig. 9 have two phases in equilibrium, (Ge) solid solution as a dark phase and L phase as a light gray phase.

The ternary system was thermodynamically assessed by CALPHAD method [29,30] using Thermo-calc software package [31].

Thermodynamic parameters for constitutive binary systems were taken from literature [20,23,24] and three vertical sections Bi-GeZn, Ge-BiZn and Zn-BiGe were extrapolated and compared with experimental data of DTA given in table 7. After comparison it is noticed that experimentally detected temperatures of liquid phase transformation are higher than calculated. By comparing EDS result of tested samples at 100 and 300 °C and extrapolated isothermal section at 100 and 300 °C it is not noticed difference in phase composition. Based on this conclusion it is noticed that it is necessary to model Liquid phase and introduce new ternary parameters for Liquid phase.

The ternary Liquid phase is treated as substitutional solution. The Gibbs free energy is expressed by the Redlich-Kister-Muggianu polynomial [32]:

$$G_m^L = x_{Bi}G_{Bi}^L + x_{Ge}G_{Ge}^L + x_{Zn}G_{Zn}^L + RT(x_{Bi}\ln x_{Bi} + x_{Ge}\ln x_{Ge} + x_{Zn}\ln x_{Zn}) + x_{Bi}x_{Ge}L_{Bi,Ge}^L$$

$$+ x_{Bi}x_{Zn}L_{Bi,Zn}^L + x_{Ge}x_{Zn}L_{Ge,Zn}^L + {}^{ex}G_{Bi,Ge,Zn}^L \quad (1)$$

where  $x_{Bi}$ ,  $x_{Ge}$  and  $x_{Zn}$  are molar fractions of elements Bi, Ge and Zn, respectively  $G_{Bi}^L$ ,  $G_{Ge}^L$  and  $G_{Zn}^L$  are the Gibbs energies of Bi, Ge and Zn in liquid phase.  $R$  is gas constant,  $T$  temperature, and  $RT(x_{Bi}\ln x_{Bi} + x_{Ge}\ln x_{Ge} + x_{Zn}\ln x_{Zn})$  corresponds to the contribution of the ideal entropy of mixing to the Gibbs energy.  $L_{Bi,Ge}^L$ ,  $L_{Bi,Zn}^L$  and  $L_{Ge,Zn}^L$  are interaction parameters from the corresponding binary systems from literature [20,23,24]. Last term in equation 1 is the ternary excess Gibbs energy, which is expressed as:

$${}^{ex}G_{Bi,Ge,Zn}^L = x_{Bi}x_{Ge}x_{Zn}(x_{Bi}{}^0L_{Bi,Ge,Zn}^L + x_{Ge}{}^1L_{Bi,Ge,Zn}^L + x_{Zn}{}^2L_{Bi,Ge,Zn}^L) \quad (2)$$

Where  ${}^0L_{Bi,Ge,Zn}^L$ ,  ${}^1L_{Bi,Ge,Zn}^L$  and  ${}^2L_{Bi,Ge,Zn}^L$  are ternary interaction parameters expressed as  ${}^iL_{Bi,Ge,Zn}^L = a_i + b_iT$ . And  $a_i$  and  $b_i$  are model parameters to be optimized from the experimental phases diagram and/or thermodynamic data.

Optimization of the parameters for liquid phase was conducted using the PARROT module [33] based on a least square procedure.

Optimization was conducted by using DTA experimental data given in Table 7 and parameters for Liquid phase.

The thermodynamic parameters for liquid phase obtained in this work are:

$${}^0L_{Bi,Ge,Zn}^L = 22601.36 - 35.07 * T \quad (3a)$$

$${}^1L_{Bi,Ge,Zn}^L = 22001.2 + 26.03 * T \quad (3b)$$

$${}^2L_{Bi,Ge,Zn}^L = -9003.1 \quad (3c)$$

By using thermodynamic data for constitutive binary systems and new ternary parameter three vertical sections, and two isothermal section were calculated in Pandat software and compared with experimental results.

Experimentally obtained results of DTA were compared with calculated vertical sections and given on Figure 10.

Figure 10. Calculated vertical sections of the ternary Bi-Ge-Zn system compared with DTA experimental results: a) Bi-GeZn, b) Ge-BiZn and c) Zn-BiGe.

Reasonable agreement between calculated and experimental results is reached. So, presented ternary parameters describe well vertical sections.

Further EDS results given in Table 8 are compared with calculated isothermal section at 100 °C.

Figure 11, presents calculated isothermal section at 100 °C compared with EDS results.

Figure 11. Calculated isothermal section at 100 °C compared with EDS results given in Table 8.

According to the calculation all tested samples are located in three-phase region (Ge)+(Zn)+(Bi) same phase region as experimentally detected with all five samples. Good agreement between experimental phase compositions and calculated composition is reached.

Figure 12, presents comparison of calculated isothermal section at 300 °C compared with EDS results given in Table 9.



Figure 12. Calculated isothermal section at 300 °C compared with EDS results given in Table 9.

Calculated isothermal section at 300 °C consists of three phase regions. Two phase regions are two-phase L+(Ge) and (Ge)+(Zn), and one is three-phase region L+(Ge)+(Zn). Compared EDS results with calculated isothermal section at 300 °C gives reasonable agreement.

Further liquidus projection was calculated and presented on Figure 13.

Figure 13. Liquidus projection of the ternary Bi-Ge-Zn system with the enlarged Bi-Zn rich region.

Predicted liquidus projection consists of four fields of primary crystallization L, (Ge), (Bi) and (Zn) and two invariant reactions (Table 10).

Table 10. Predicted invariant reaction of the ternary Bi-Ge-Zn system.

## 5. Conclusion

Two ternary systems are experimentally tested by DTA, SEM-EDS and XRD methods. In these ternary systems by EDS test are not detect any new compounds. EDS results were compared with calculated isothermal section at 100 °C and 300 °C, and good agreement is reached. DTA results of 12 samples in both ternary systems were compared with corresponding calculated vertical sections and good agreement is reached for Bi-Ge-Ga systems while for ternary Bi-Ge-Zn experimental liquidus temperatures were higher. For good description of ternary Bi-Ge-Zn it was necessary to introduce new ternary parameters for liquid phase. By adding new parameters good description of the ternary system has been reached.

## Acknowledgements

This work has been supported by the Ministry of Education, Science and Technological Development of the Republic of Serbia (Grant No. OI172037).

## References

- [1] S. Raoux, T.J. Ibm, Phase Change Memory (PCM) Materials and Devices, Advances in Nonvolatile Memory and Storage Technology, 2nd ed., Y. Nishi, Ed., Elsevier, Amsterdam, (2014) 161–199. <https://doi.org/10.1533/9780857098092.2.161>
- [2] A.V. Kolobov, J. Tominaga, P. Fons, Phase-change memory materials, in: S. Kasap, P. Capper (Eds.), Springer Handbook of Electronic and Photonic Materials, Springer Handbooks. Springer, Cham, 2017. [https://doi.org/10.1007/978-3-319-48933-9\\_46](https://doi.org/10.1007/978-3-319-48933-9_46)
- [3] N. Yamada, E. Ohno, N. Akahira, K. Nishiuchi, K. Nagata, M. Takao, High Speed Over Writable Phase Change Optical Disk Material, Jpn. J. Appl. Phys., 26 (1987) 61–66. <https://doi.org/10.7567/JJAPS.26S4.61>
- [4] Y.C. Chen, C.T. Rettner, S. Raoux, G.W. Burr, S.H. Chen, R.M. Shelby, M. Salinga, W. Risk, T.D. Happ, G.M. McClelland, M. Breitwisch, A. Schrott, J.B. Philipp, M.H. Lee, R. Cheek, T. Nirschl, M. Lamorey, C.F. Chen, E. Joseph, S. Zaidi, B. Yee, H.L. Lung, R. Bergmann, C. Lam, IEEE Int. Electron Dev. Mtg. 777 (2006) San Francisco, CA.
- [5] T. Siegrist, P. Jost, H. Volker, M. Woda, P. Merkelbach, C. Schlockermann, M. Wuttig, Disorder-Induced Localization in Crystalline Phase-Change Materials, Nat. Mater., 10 (2011) 202–208. <https://doi.org/10.1038/nmat2934>
- [6] S. Adachi, Properties of Semiconductor Alloys: Group-IV, III-V and II-VI, Semiconductors, Wiley, Hoboken, 2009

- [7] A. Rockett, *The Materials Science of Semiconductors*, Springer, Berlin, 2008
- [8] G.W. Burr, B.N. Kurdi, J.C. Scott, C.H. Lam, K. Gopalakrishnan, R.S. Shenoy, Overview of candidate device technologies for storage-class memory, *IBM J. Res. Dev.*, 52(4–5) (2008) 449–464. <https://doi.org/10.1147/rd.524.0449>
- [9] T.C. Chong, X. Hu, L.P. Shi, P.K. Tan, X.S. Miao, R. Zhao, Multispeed Superlattice-Like Phase Change Optical Disk, *Jpn. J. Appl. Phys.*, 42 (2B) (2003) 824–827. <https://doi.org/10.1143/JJAP.42.824>
- [10] E. Dichia, A. Wojakowskab, B. Legendrea, Study of the ternary system germanium–antimony–tin: experimental phase diagram, *J. Alloys Compd.*, 320 (2001) 218–223. [https://doi.org/10.1016/S0925-8388\(00\)01489-4](https://doi.org/10.1016/S0925-8388(00)01489-4)
- [11] J. Solis, C.N. Afonso, J.F. Trull, M.C. Morilla, Fast crystallizing GeSb alloys for optical data storage, *J. Appl. Phys.*, 75(12) (1994) 7788–7793. <https://doi.org/10.1063/1.356584>
- [12] V. Tomashyk, *Ternary Alloys Based on III-V Semiconductors* (CRC Press, 2017). ISBN 9781498778381
- [13] L. Tichý, H. Tichá, A. Pačesová, J. Petzelt, On the infrared spectra of Ge-Bi-Se(S) glasses, *J. Non-Cryst. Solids.*, 128(2) (1991) 191-196. [https://doi.org/10.1016/0022-3093\(91\)90513-6](https://doi.org/10.1016/0022-3093(91)90513-6)
- [14] A. Djordjević, D. Minić, M. Premović, D. Manasijević, V. Čosović, Experimental Examination and Thermodynamic Description of the Ternary Bi-Ge-In and -Sn Systems, *J. Phase Equilib. Diffus.*, (2019) <https://doi.org/10.1007/s11669-019-00749-5>.
- [15] M. Premović, D. Minić, V. Cosović, D. Manasijević, D. Živković, Experimental investigation and thermodynamic calculations of the Bi-Ge-Sb phase diagram, *Metall. Mater. Trans A*, 45A (2014) 4829-4841. <https://doi.org/10.1007/s11661-014-2445-4>

- [16] H. P. Trah, Liquid phase epitaxy in the ternary system Si-Ge-Bi, *J Cryst Growth.*, 102(1-2) (1990) 175-182. [https://doi.org/10.1016/0022-0248\(90\)90899-V](https://doi.org/10.1016/0022-0248(90)90899-V)
- [17] D. Milisavljević, D. Minić, M. Premović, D. Manasijević, V. Čosović, N. Košanin, Combined thermodynamic description and experimental investigation of the ternary Ag-Bi-Ge system, *Int J Thermophys.*, 40 (2019) 29. <https://doi.org/10.1007/s10765-019-2495-3>
- [18] P. Fima, A. Gazda, Thermal Analysis of Selected Sn-Ag-Cu Alloys, *J. Therm. Anal. Calorim.*, 112 (2013) 731-737. <https://doi.org/10.1007/s10973-012-2583-0>
- [19] W.J. Boettinger, U.R. Kattner, K.W. Moon, J.H. Perepezko, in *DTA and Heat-Flux DSC Measurements of Alloy Melting and Freezing (NIST recommended practice guide, Special publication 960-15, NIST, 2006)*. <https://doi.org/10.6028/NBS.SP.960-15>
- [20] P.Y. Chevalier, Thermodynamic evaluation of the Bi-Ge system, *Thermochim. Acta*, 132 (1988) 111–116. [https://doi.org/10.1016/0040-6031\(88\)87100-4](https://doi.org/10.1016/0040-6031(88)87100-4)
- [21] C. Girard, Excess functions and equilibrium phase diagrams of four ternary metallic systems: Al-Ga-In, Al-Bi-Ga, Bi-Ga-Zn, Al-Ga-Sb (in French), Thesis University of Provence, Marseille, France, 1985
- [22] R. W. Olesinski, G. J. Abbaschian, The Ga–Ge (Gallium-Germanium) system, *Binary of Alloy Phase Diagrams*, 6(3) (1985) 258–262. <https://doi.org/10.1007/BF02880411>
- [23] Dmitri V. Malakhov, Thermodynamic assessment of the Bi-Zn system, *Calphad*, 24 (2000) 1-14. [https://doi.org/10.1016/S0364-5916\(00\)00011-0](https://doi.org/10.1016/S0364-5916(00)00011-0)
- [24] P. Y. Chevalier, A thermodynamic evaluation of the Germanium-Indium, Germanium-Lead, Germanium-Antimony, Germanium-Thallium and Germanium Zinc systems, *Thermochim Acta.*, 155 (1989) 227-240. DOI: [10.1016/0040-6031\(89\)87148-5](https://doi.org/10.1016/0040-6031(89)87148-5)

- [25] A. S. Cooper, Precise lattice constants of germanium, aluminum, gallium arsenide, uranium, sulphur, quartz and sapphire, *Acta Cryst.* 15 (1962) 578–582. <https://doi.org/10.1107/S0365110X62001474>
- [26] P. Cucka, C. S. Barrett, The crystal structure of Bi and of solid solutions of Pb, Sn, Sb and Te in Bi, *Acta Cryst.*, 15 (1962) 865-872. <https://doi.org/10.1107/S0365110X62002297>
- [27] B. D. Sharma, J. Donohue, A refinement of the crystal structure of gallium, *Cryst. Mater.* (1962) 293-300. <https://doi.org/10.1524/zkri.1962.117.4.293>
- [28] N. Ridley, Densities of some indium solid solutions, *J. Less Common. Met.* 8 (1965) 354–357. [https://doi.org/10.1016/0022-5088\(65\)90071-8](https://doi.org/10.1016/0022-5088(65)90071-8)
- [29] N. Saunders, A.P. Miodownik, CALPHAD (calculation of phase diagrams): a comprehensive guide, Pergamon Materials Series 1, Elsevier Science Ltd, The Boulevard, Langford Lane, Kidlington, Oxford OX5 1GB, United Kingdom, London, 1998.
- [30] H.L. Lukas, S.G. Fries, B. Sundman, Computational Thermodynamics: CALPHAD Method, Cambridge University Press, Cambridge, UK, 2007. <https://doi.org/10.1017/CBO9780511804137>
- [31] B. Sundman, B. Jansson, J.O. Andersson, The thermo-calc databank system, *Calphad.* 9 (1985) 153–190. [https://doi.org/10.1016/0364-5916\(85\)90021-5](https://doi.org/10.1016/0364-5916(85)90021-5).
- [32] O. Redlich, A.T. Kister, Thermodynamics of nonelectrolytic solutions. Algebraic representation of thermodynamic properties and the classification of solutions, *Ind. Eng. Chem.* 40 (1948) 84–88. <https://doi.org/10.1021/ie50457a601>.
- [33] B. Jansson, Tricta-Mac-0234, Royal Institute of Technology, Stockholm, Sweden, 1984.

Figure 1. Calculated binary phase diagrams a) Bi-Ge system [14], b) Bi-Ga system [15], c) Ga-Ge system [16], d) Bi-Zn system [17] and e) Ge-Zn system [18].

Figure 2. Calculated vertical sections of the ternary Bi-Ga-Ge system compared with DTA experimental results: a) Bi-GaGe, b) Ge-BiGa and c) Ga-BiGe.

Figure 3. SEM micrographs of sample 2.

Figure 4. Calculated isothermal section at 100 °C compared with EDS results given in Table 3.

Figure 5. SEM micrographs of sample 4.

Figure 6. Calculated isothermal section at 300 °C compared with EDS results given in Table 4.

Figure 7. Liquidus projection of the ternary Bi-Ga-Ge system with the enlarged Bi-Ga rich region.

Figure 8. SEM micrograph of sample 2.

Figure 9. SEM micrograph of sample 4.

Figure 10. Calculated vertical sections of the ternary Bi-Ge-Zn system compared with DTA experimental results: a) Bi-GeZn, b) Ge-BiZn and c) Zn-BiGe.

Figure 11. Calculated isothermal section at 100 °C compared with EDS results given in Table 7.

Figure 12. Calculated isothermal section at 300 °C compared with EDS results given in Table 8.

Figure 13. Liquidus projection of the ternary Bi-Ge-Zn system with the enlarged Bi-Zn rich region.

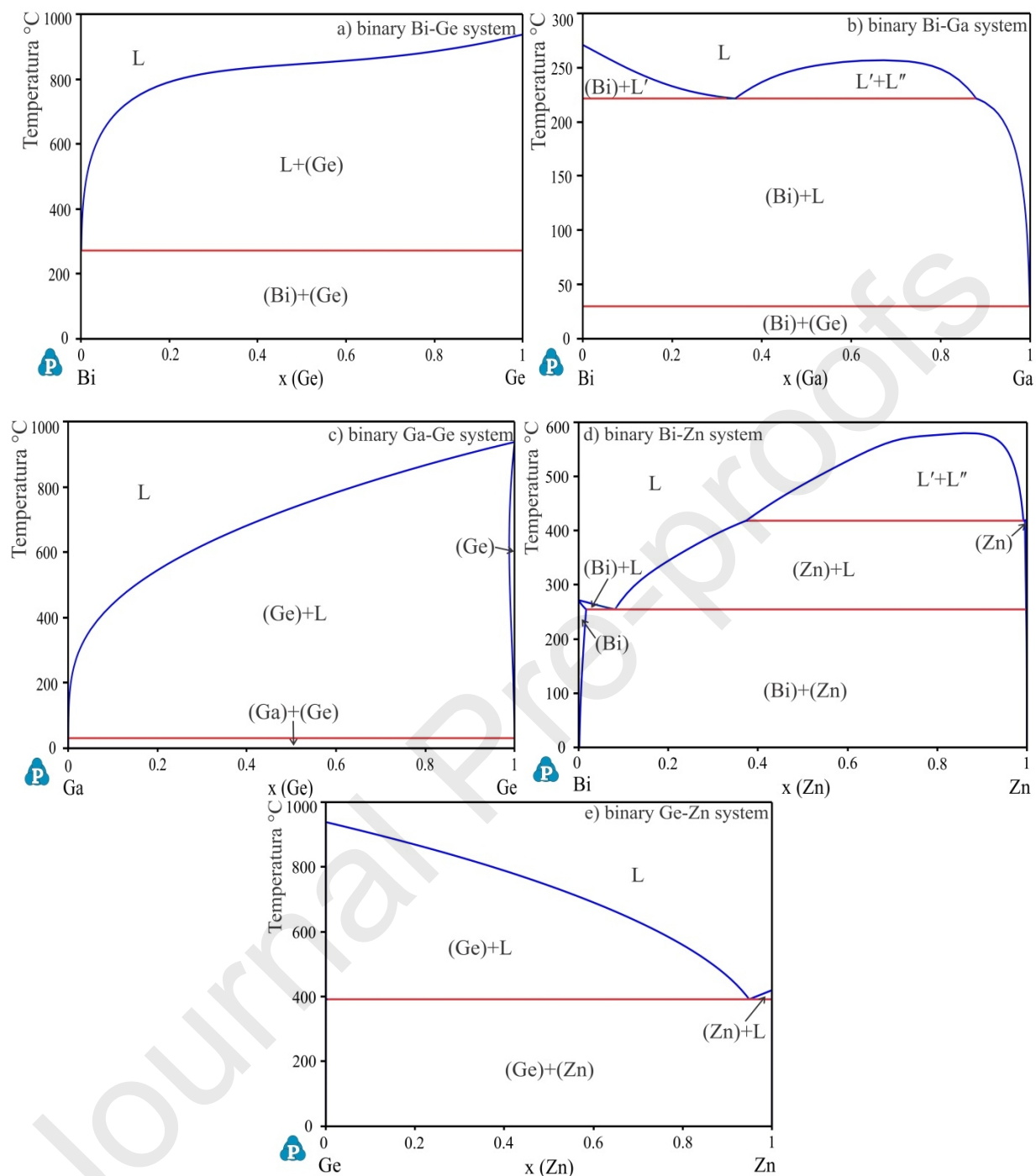


Figure 1. Calculated binary phase diagrams a) Bi-Ge system [14], b) Bi-Ga system [15], c) Ga-Ge system [16], d) Bi-Zn system [17] and e) Ge-Zn system [18].

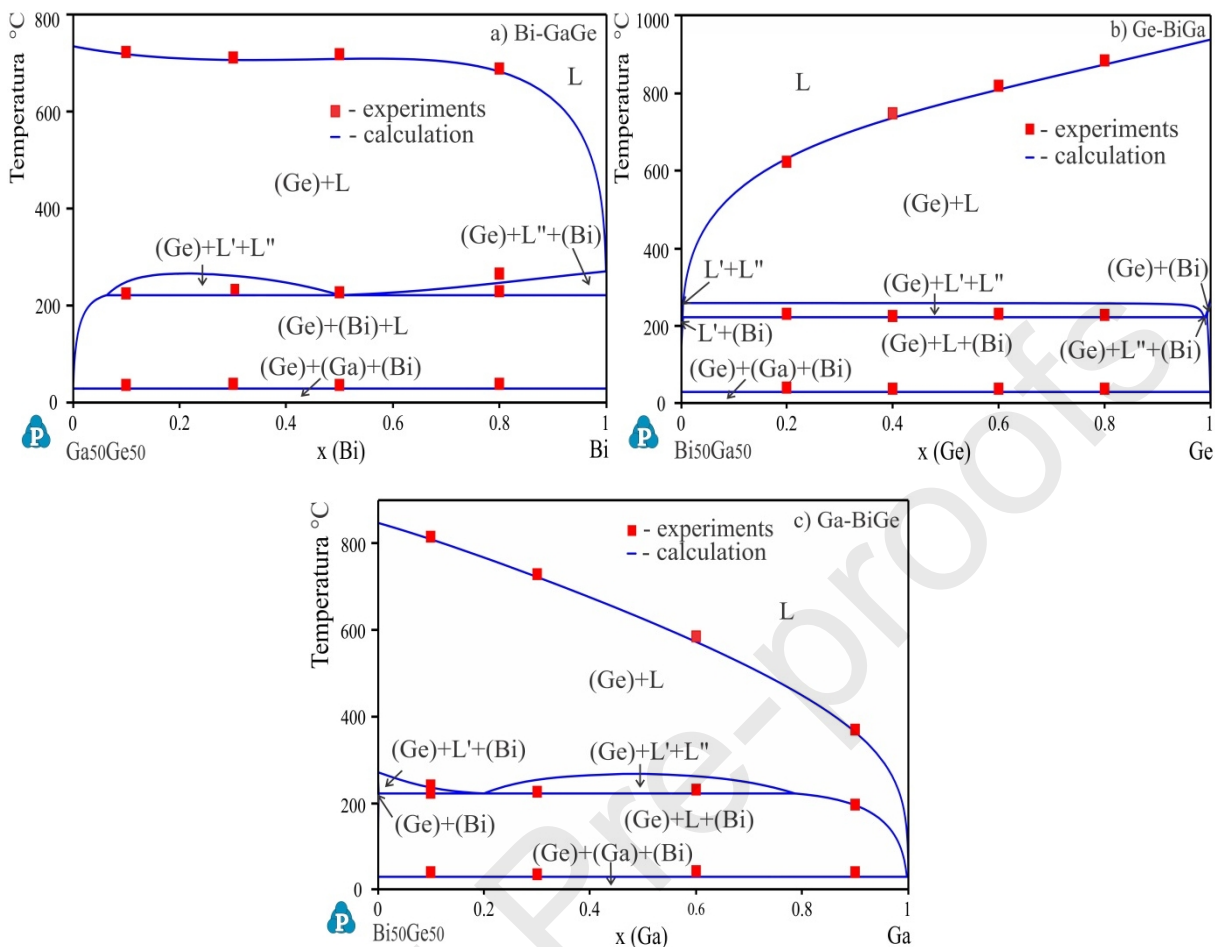


Figure 2. Calculated vertical sections of the ternary Bi-Ga-Ge system compared with DTA experimental results: a) Bi-GaGe, b) Ge-BiGa and c) Ga-BiGe.

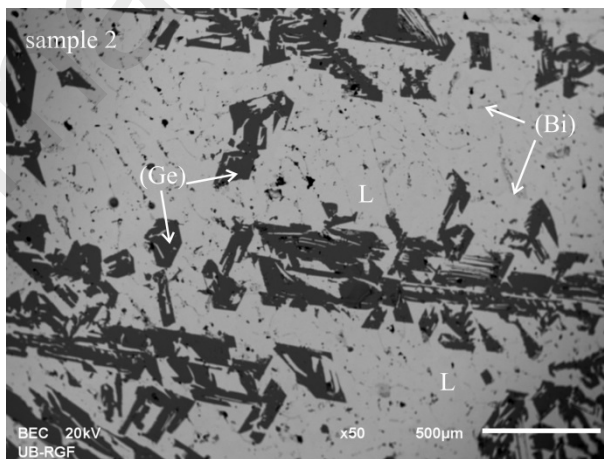


Figure 3. SEM micrographs of sample 2.



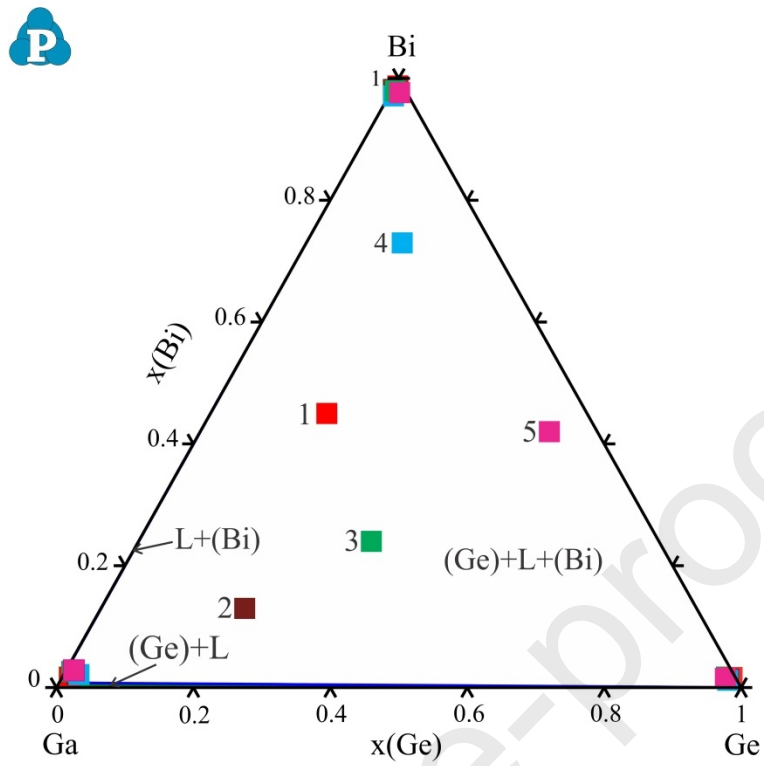


Figure 4. Calculated isothermal section at 100 °C compared with EDS results given in Table 3.

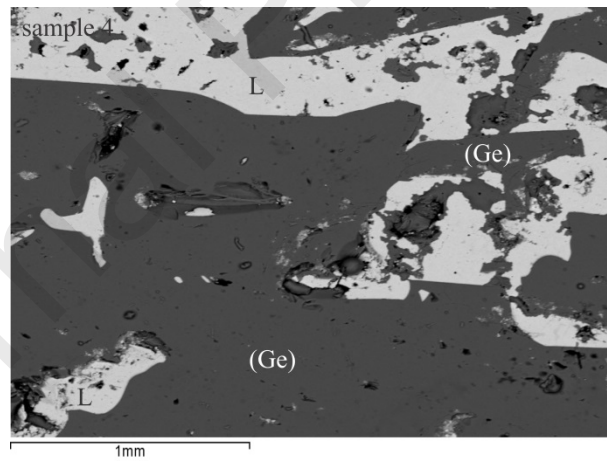


Figure 5. SEM micrographs of sample 4.

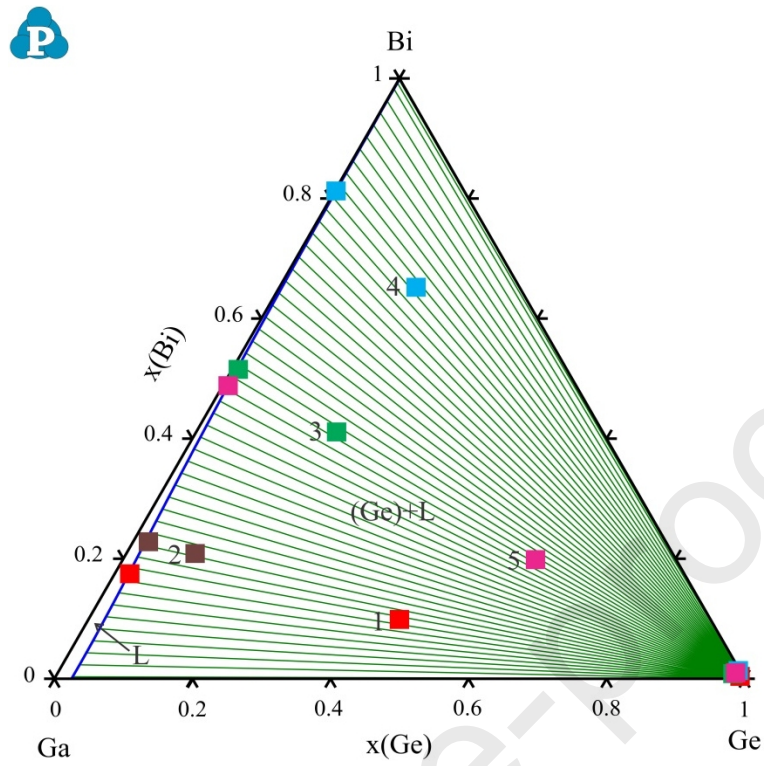


Figure 6. Calculated isothermal section at 300 °C compared with EDS results given in Table 4.

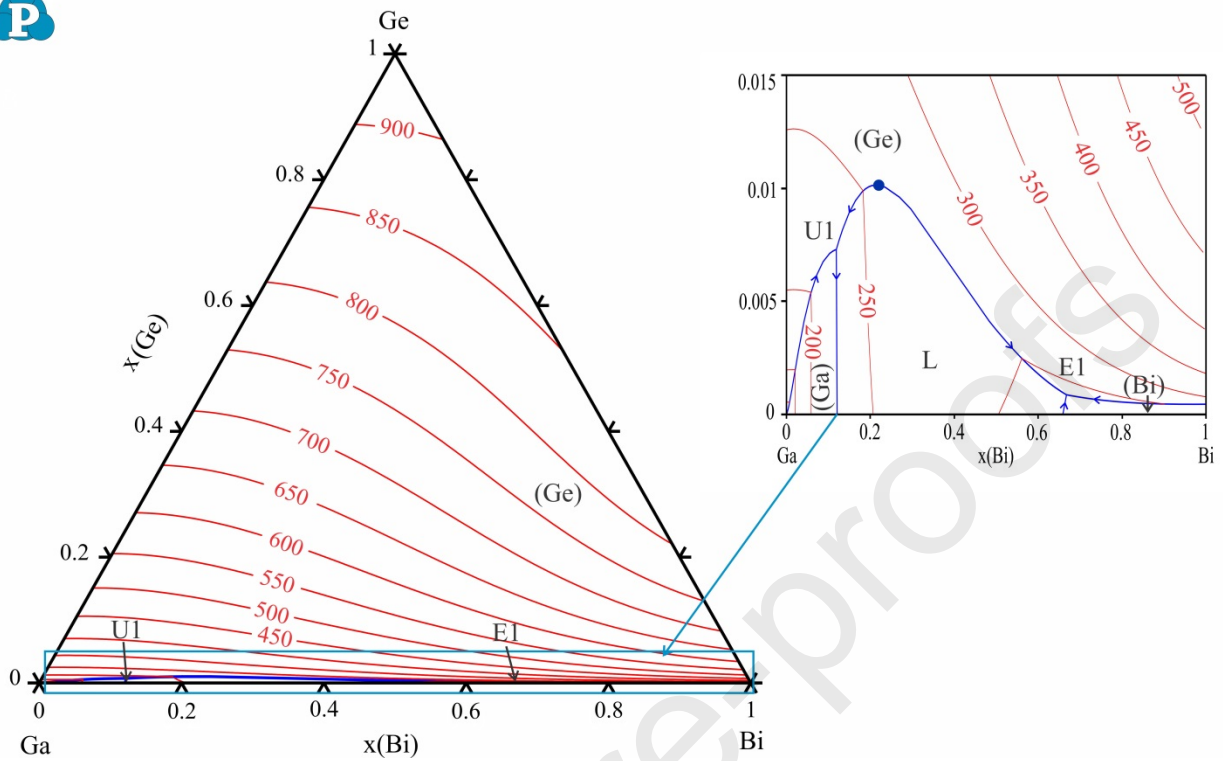


Figure 7. Liquidus projection of the ternary Bi-Ga-Ge system with the enlarged Bi-Ga rich region.

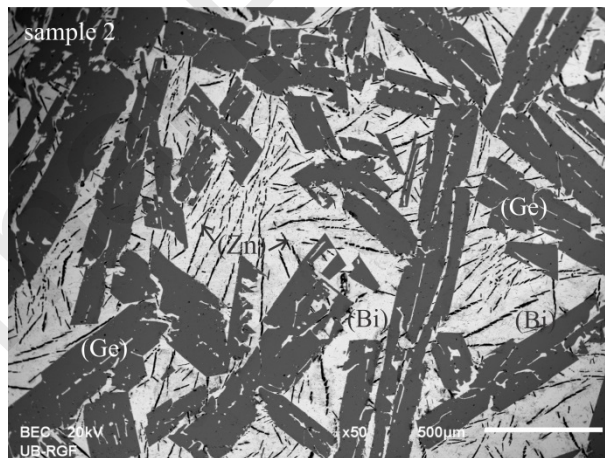


Figure 8. SEM micrograph of sample 2.

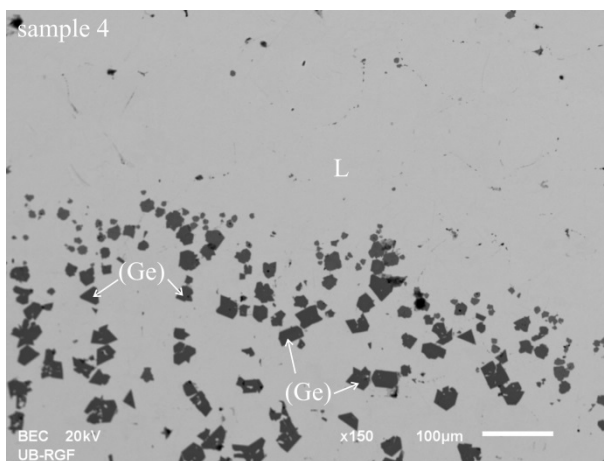


Figure 9. SEM micrograph of sample 4.

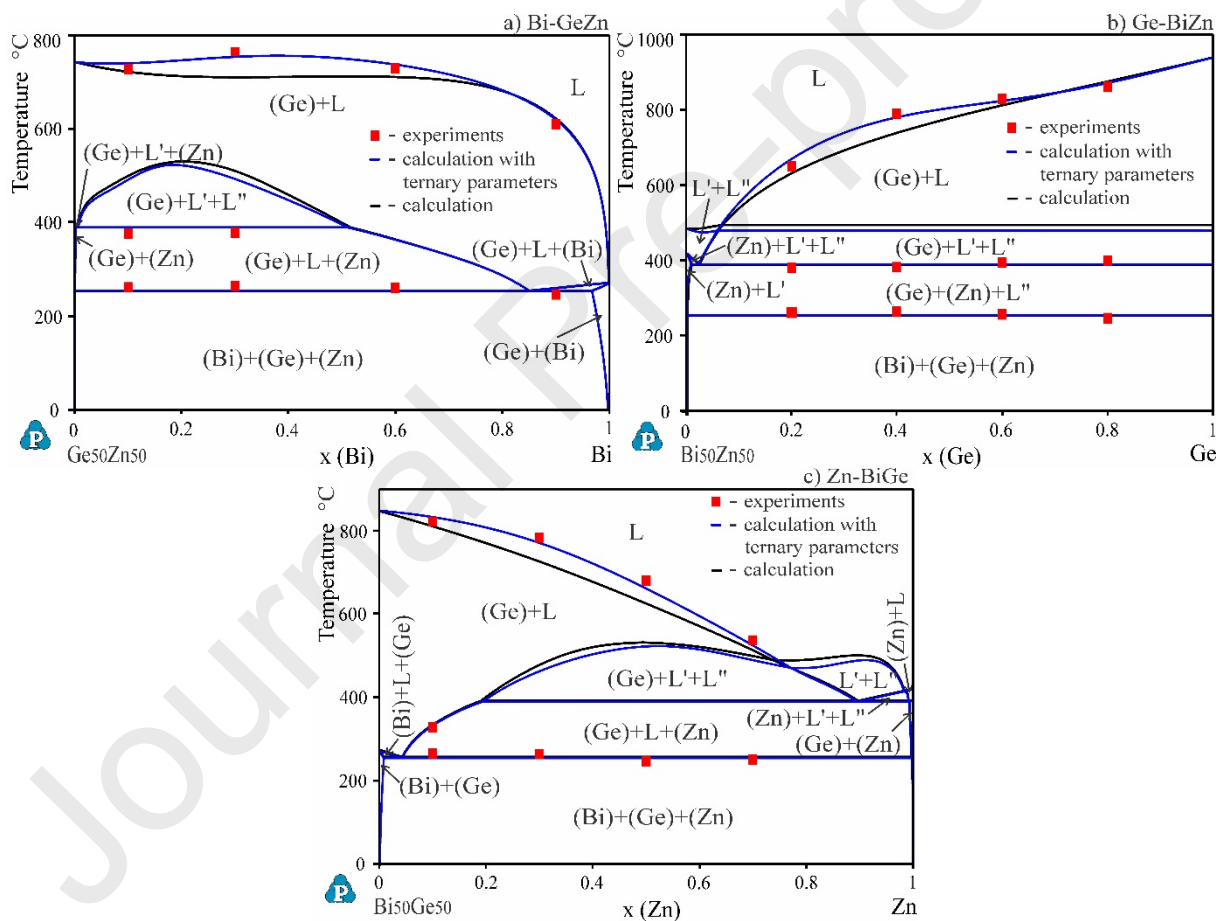


Figure 10. Calculated vertical sections of the ternary Bi-Ge-Zn system compared with DTA experimental results: a) Bi-GeZn, b) Ge-BiZn and c) Zn-BiGe.

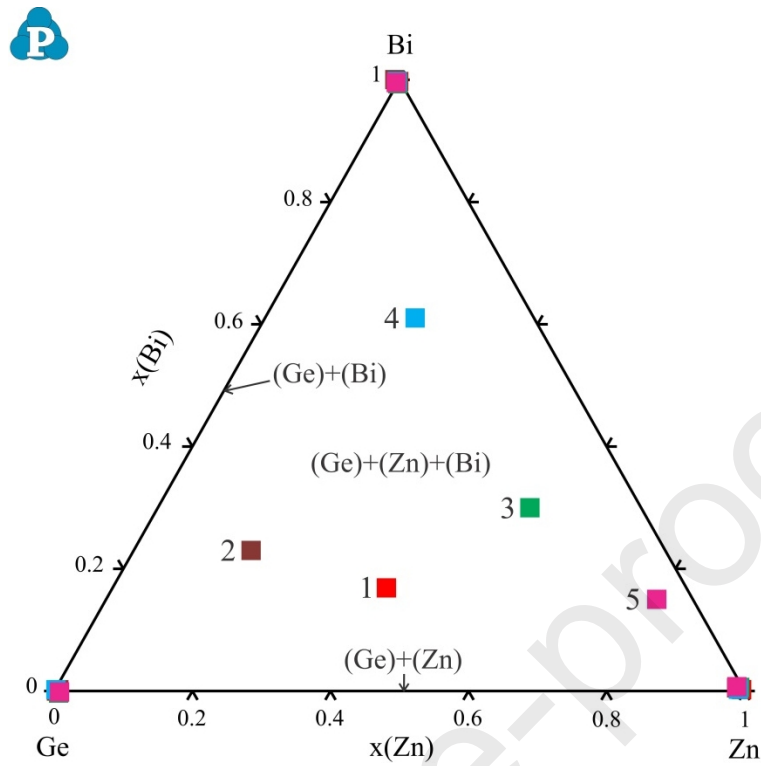


Figure 11. Calculated isothermal section at 100 °C compared with EDS results given in Table 7.

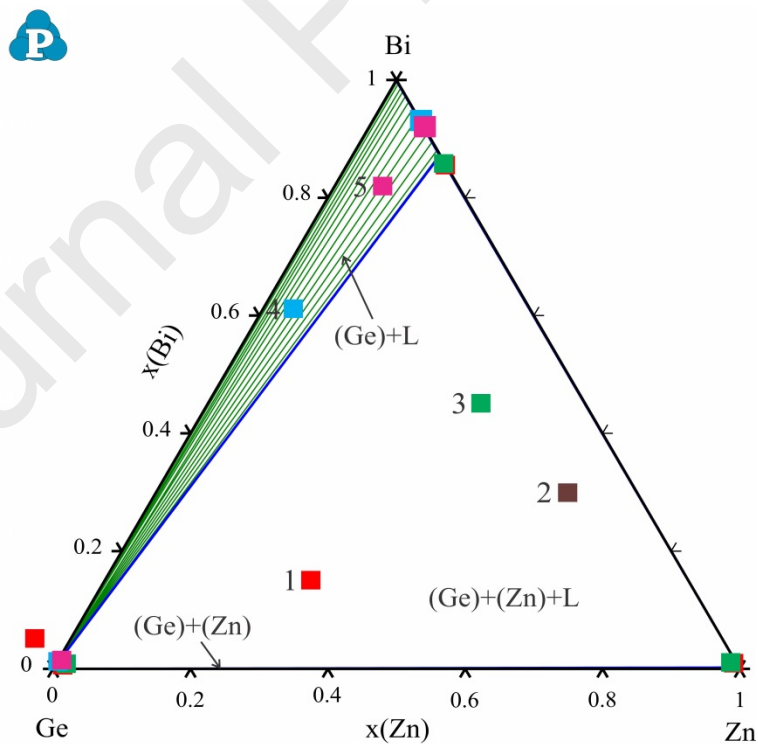


Figure 12. Calculated isothermal section at 300 °C compared with EDS results given in Table 8.

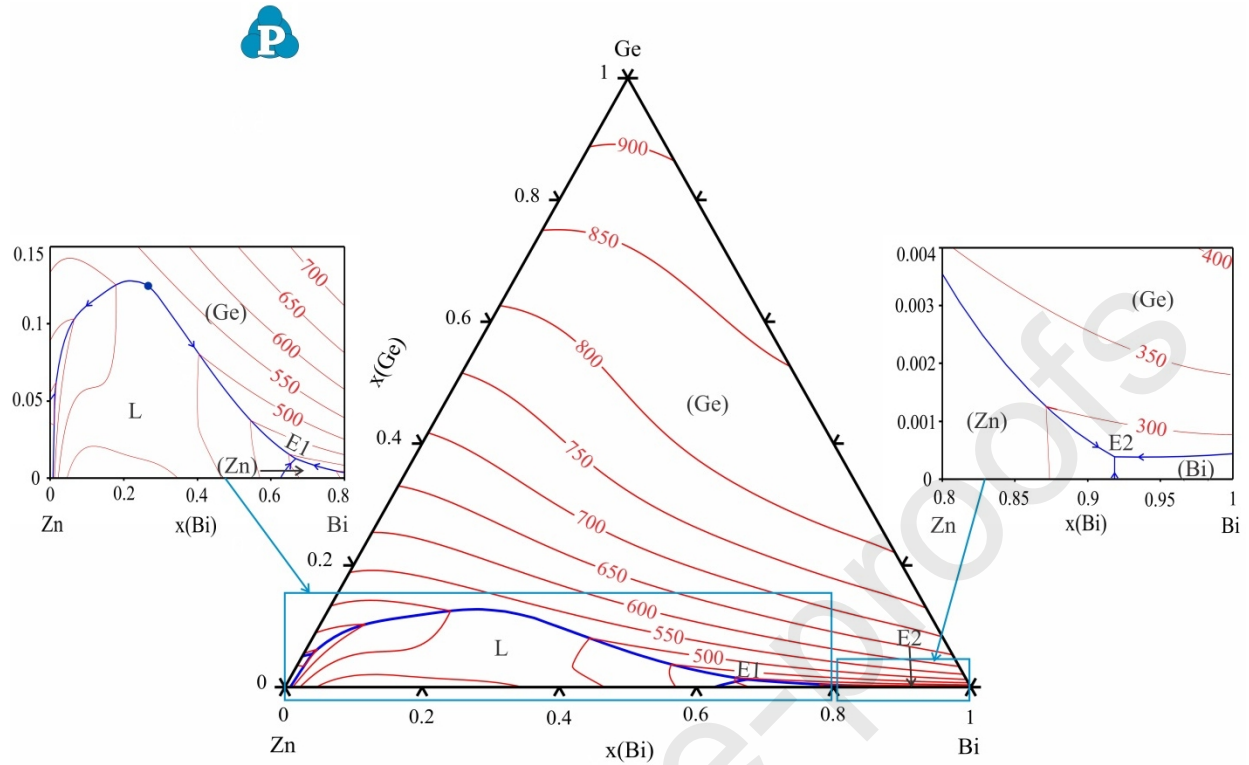


Figure 13. Liquidus projection of the ternary Bi-Ge-Zn system with the enlarged Bi-Zn rich region.

Table 1. Sample table with the purities provided by the supplier

Table 2. Considered phase, their crystallographic data and database names for the phases of the ternary Bi-Ga-Ge and Bi-Ge-Zn systems.

Table 3. Phase transition temperatures of the studied alloys from the ternary Bi-Ga-Ge system determined by DTA at pressure  $p=0.1$  MPa<sup>a</sup>.

Table 4. Combined results of SEM-EDS and XRD analyzes of the selected Bi-Ga-Ge alloys annealed at  $T=100$  °C (standard uncertainty (u):  $u(T)=1.0$  °C) at pressure  $p=0.1$  MPa (standard uncertainty (u):  $u(p)=1$  kPa).

Table 5 Combined results of SEM-EDS and XRD analyzes of the selected Bi-Ga-Ge alloys annealed at  $T=300$  °C (standard uncertainty (u):  $u(T)=1.0$  °C) at pressure  $p=0.1$  MPa (standard uncertainty (u):  $u(p)=1$  kPa).

Table 6. Predicted invariant reaction of the ternary Bi-Ga-Ge system.

Table 7. Phase transition temperatures of the studied alloys from the ternary Bi-Ge-Zn system determined by DTA at pressure  $p=0.1$  MPa<sup>a</sup>.

Table 8. Combined results of SEM-EDS and XRD analyzes of the selected Bi-Ge-Zn alloys annealed at  $T=100$  °C (standard uncertainty (u):  $u(T)=1.0$  °C) at pressure  $p=0.1$  MPa (standard uncertainty (u):  $u(p)=1$  kPa).

Table 9. Combined results of SEM-EDS and XRD analyzes of the selected Bi-Ge-Zn alloys annealed at  $T=300$  °C (standard uncertainty (u):  $u(T)=1.0$  °C) at pressure  $p=0.1$  MPa (standard uncertainty (u):  $u(p)=1$  kPa).

Table 10. Predicted invariant reaction of the ternary Bi-Ge-Zn system.

Table 1. Sample table with the purities provided by the supplier

Chemical name	Source/stock no.	Initial purity x(at.%)
Bi rod	Alfa Aesar/ 35854	99.999
Ge pieces	Alfa Aesar/10191	99.999
Zn ingot	Alfa Aesar/00420	99.999
Ga ingot	Alfa Aesar/ 10187	99.999

Table 2. Considered phase, their crystallographic data and database names for the phases of the ternary Bi-Ga-Ge and Bi-Ge-Zn systems.

Thermodynamic database name	Phase	Pearson symbol	Space group	Lattice parameters (Å) <sup>a</sup>			Ref.
				<i>a</i>	<i>b</i>	<i>c</i>	
LIQUID	Liquid	-	-				
DIAMOND_A4	(Ge)	<i>cF8</i>	<i>Fd<math>\bar{3}m</math></i>	5.65675±0.00003			[25]
RHOMBO_A7	(Bi)	<i>hR2</i>	<i>R<math>\bar{3}m</math></i>	4.535±0.002	4.535±0.002	11.814±0.006	[26]
ORTHORHOMBIC_GA	(Ga)	<i>oS8</i>	<i>Cmca</i>	4.5197±0.0001	7.6633±0.0002	4.5260±0.0003	[27]
HCP_ZN	(Zn)	<i>hP2</i>	<i>P6<math>_3</math>/mmc</i>	2.665±0.002		4.947±0.0001	[28]

<sup>a</sup> Uncertainties reported inside the table are standard uncertainties, (0.68 level of confidence).

Table 3. Phase transition temperatures of the studied alloys from the ternary Bi-Ga-Ge system determined by DTA at pressure p=0.1 MPa<sup>a</sup>.

Composition (at.%)		1. identified phase transition		2. identified phase transition		3. identified phase transition	
nominal	EDS <sup>a</sup>	Ternary eutectic reaction temperature (°C) <sup>a</sup>	Coexisting phases	Ternary transition reaction temperature (°C) <sup>a</sup>	Coexisting phases	Liquidus temperature (°C) <sup>a</sup>	Coexisting phases
Vertical section Bi-GaGe							
Bi <sub>10</sub> Ga <sub>45</sub> Ge <sub>45</sub>	Bi <sub>10.03</sub> Ga <sub>44.01</sub> Ge <sub>45.96</sub>	34.3	L', (Ge), (Ga), (Bi)	226.8	L', L'', (Ge), (Bi)	724.3	L, (Ge)
Bi <sub>30</sub> Ga <sub>35</sub> Ge <sub>35</sub>	Bi <sub>29.18</sub> Ga <sub>35.32</sub> Ge <sub>35.50</sub>	35.8	L', (Ge), (Ga), (Bi)	230.3	L', L'', (Ge), (Bi)	712.0	L, (Ge)
Bi <sub>50</sub> Ga <sub>25</sub> Ge <sub>25</sub>	Bi <sub>50.93</sub> Ga <sub>23.97</sub> Ge <sub>25.10</sub>	33.1	L', (Ge), (Ga), (Bi)	227.1	L', L'', (Ge), (Bi)	719.6	L, (Ge)
Bi <sub>80</sub> Ga <sub>10</sub> Ge <sub>10</sub>	Bi <sub>80.92</sub> Ga <sub>8.71</sub> Ge <sub>10.37</sub>	34.9	L', (Ge), (Ga), (Bi)	229.2	L', L'', (Ge), (Bi)	689.8	L, (Ge)
Vertical section Ga-BiGe							
Bi <sub>45</sub> Ga <sub>10</sub> Ge <sub>45</sub>	Bi <sub>44.92</sub> Ga <sub>9.13</sub> Ge <sub>45.95</sub>	35.9	L', (Ge), (Ga), (Bi)	224.3	L', L'', (Ge), (Bi)	815.4	L, (Ge)
Bi <sub>35</sub> Ga <sub>30</sub> Ge <sub>35</sub>	Bi <sub>35.67</sub> Ga <sub>29.71</sub> Ge <sub>34.62</sub>	32.9	L', (Ge), (Ga), (Bi)	226.1	L', L'', (Ge), (Bi)	729.5	L, (Ge)
Bi <sub>20</sub> Ga <sub>60</sub> Ge <sub>20</sub>	Bi <sub>19.52</sub> Ga <sub>60.03</sub> Ge <sub>20.45</sub>	37.6	L', (Ge), (Ga), (Bi)	231.4	L', L'', (Ge), (Bi)	585.2	L, (Ge)
Bi <sub>5</sub> Ga <sub>90</sub> Ge <sub>5</sub>	Bi <sub>5.71</sub> Ga <sub>89.32</sub> Ge <sub>4.97</sub>	36.8	L', (Ge), (Ga), (Bi)	196.9 (monovariant transition)	L', (Ge), (Bi)	370.8	L, (Ge)
Vertical section Ge-BiGa							
Bi <sub>40</sub> Ga <sub>40</sub> Ge <sub>20</sub>	Bi <sub>40.73</sub> Ga <sub>39.92</sub> Ge <sub>19.35</sub>	36.4	L', (Ge),	231.6	L', L'',	624.5	L, (Ge)



			(Ga), (Bi)		(Ge), (Bi)		
Bi <sub>30</sub> Ga <sub>30</sub> Ge <sub>40</sub>	Bi <sub>29.76</sub> Ga <sub>29.13</sub> Ge <sub>41.11</sub>	35.1	L', (Ge), (Ga), (Bi)	226.6	L', L'', (Ge), (Bi)	748.5	L, (Ge)
Bi <sub>20</sub> Ga <sub>20</sub> Ge <sub>60</sub>	Bi <sub>19.67</sub> Ga <sub>20.87</sub> Ge <sub>59.46</sub>	36.1	L', (Ge), (Ga), (Bi)	231.9	L', L'', (Ge), (Bi)	820.4	L, (Ge)
Bi <sub>10</sub> Ga <sub>10</sub> Ge <sub>80</sub>	Bi <sub>10.08</sub> Ga <sub>9.52</sub> Ge <sub>80.40</sub>	33.5	L', (Ge), (Ga), (Bi)	227.6	L', L'', (Ge), (Bi)	884.6	L, (Ge)

<sup>a</sup>Standard uncertainty (u) (0.68 level of confidence) calculated from repeated DTA measurements: for invariant reactions:  $u(T)=1.5$  °C; for monovariant phase transition:  $u(T)=2.8$  °C; for liquidus temperatures:  $u(T)=5.1$  °C;  $u(p)=1$  kPa;  $u(x)=0.1$  at. %

Table 4. Combined results of SEM-EDS and XRD analyzes of the selected Bi-Ga-Ge alloys annealed at  $T=100$  °C (standard uncertainty (u):  $u(T)=1.0$  °C) at pressure  $p=0.1$  MPa (standard uncertainty (u):  $u(p)=1$  kPa).

N.	Composition of samples (at. %) <sup>a</sup>	Determined phases		Compositions of phases (at. %) <sup>b</sup>			Lattice parameters (Å) <sup>b</sup>	
		SEM-EDS	XRD	Bi	Ga	Ge	$a=b$	$c$
1	45.11 Bi	(Bi)	(Bi)	99.32±0.2	0.16±0.5	0.52±0.2	4.5567±0.0006	11.8253±0.0003
	37.91 Ga	L		1.09±0.3	98.57±0.2	0.34±0.8		
	16.98 Ge	(Ge)	(Ge)	0.63±0.5	0.22±0.7	99.15±0.7	5.6572±0.0004	
2	13.02 Bi	(Bi)	(Bi)	98.85±0.7	0.40±0.1	0.75±0.4	4.5341±0.0002	11.8231±0.0001
	65.97 Ga	L		1.32±0.1	98.26±0.3	0.42±0.2		
	21.01 Ge	(Ge)	(Ge)	0.86±0.5	0.51±0.5	98.63±0.5	5.6543±0.0004	
3	23.99 Bi	(Bi)	(Bi)	99.32±0.2	0.37±0.3	0.31±0.5	4.5567±0.0001	11.8252±0.0006
	41.94 Ga	L		1.32±0.3	98.46±0.5	0.22±0.4		
	34.07 Ge	(Ge)	(Ge)	0.86±0.1	0.10±0.6	99.04±0.3	5.6565±0.0003	
4	73.01 Bi	(Bi)	(Bi)	98.85±0.3	0.61±0.6	0.54±0.2	4.5342±0.0003	11.8229±0.0003
	12.94 Ga	L		1.55±0.3	97.94±0.2	0.51±0.1		
	14.05 Ge	(Ge)	(Ge)	0.86±0.5	0.51±0.3	98.63±0.5	5.6541±0.0006	
5	42.08 Bi	(Bi)	(Bi)	98.85±0.2	0.81±0.5	0.34±0.7	4.5343±0.0002	11.8230±0.0002
	7.36 Ga	L		1.55±0.3	97.94±0.1	0.51±0.5		
	50.56 Ge	(Ge)	(Ge)	0.86±0.5	0.10±0.3	99.04±0.4	5.6563±0.0007	

<sup>a</sup>Standard uncertainty  $u(x)=0.1$  at. % (0.68 level of confidence).

<sup>b</sup>Uncertainties reported inside the table are standard uncertainties, (0.68 level of confidence).

Table 5 Combined results of SEM-EDS and XRD analyzes of the selected Bi-Ga-Ge alloys annealed at  $T=300$  °C (standard uncertainty (u):  $u(T)=1.0$  °C) at pressure  $p=0.1$  MPa (standard uncertainty (u):  $u(p)=1$  kPa).

N.	Composition of samples (at. %) <sup>a</sup>	Determined phases		Compositions of phases (at. %) <sup>b</sup>			Lattice parameters (Å) <sup>b</sup>
		SEM-EDS	XRD	Bi	Ga	Ge	$a=b=c$
1	11.01 Bi	L		18.46±0.2	79.63±0.5	1.91±0.2	5.6529±0.0003
	44.01 Ga	(Ge)	(Ge)	0.86±0.5	0.10±0.7	99.04±0.7	
	44.98 Ge						
2	21.02 Bi	L		23.71±0.7	74.58±0.1	1.71±0.4	5.6533±0.0006
	68.97 Ga	(Ge)	(Ge)	0.86±0.5	0.51±0.5	98.63±0.5	
	10.01 Ge						
3	40.99 Bi	L		50.98±0.2	48.27±0.3	0.75±0.5	5.6563±0.0008
	38.94 Ga	(Ge)	(Ge)	0.63±0.1	0.22±0.6	99.15±0.3	
	20.07 Ge						
4	65.08 Bi	L		82.24±0.3	17.72±0.6	0.04±0.2	5.6543±0.0001
	14.87 Ga	(Ge)	(Ge)	0.86±0.5	0.51±0.3	98.63±0.5	
	20.05 Ge						
5	20.02 Bi	L		46.57±0.2	52.53±0.5	0.90±0.7	5.6554±0.0002
	19.42 Ga	(Ge)	(Ge)	0.86±0.5	0.10±0.3	99.04±0.4	
	60.56 Ge						

<sup>a</sup>Standard uncertainty  $u(x)=0.1$  at. % (0.68 level of confidence).

<sup>b</sup>Uncertainties reported inside the table are standard uncertainties, (0.68 level of confidence).

Table 6. Predicted invariant reaction of the ternary Bi-Ga-Ge system.

T (°C)	Reaction	Type	Composition (mol)		
			x(Bi)	x(Ga)	x(Ge)
222.14	$L+(Ge) \rightarrow (Bi)+L$	U1	0.6674	0.3317	0.0009
29.57	$L \rightarrow (Bi)+(Ge)+(Ga)$	E1	0.0013	0.9986	0.0001

Table 7. Phase transition temperatures of the studied alloys from the ternary Bi-Ge-Zn system determined by DTA at pressure  $p=0.1$  MPa<sup>a</sup>.

Composition (at.%)		1. identified phase transition		2. identified phase transition		3. identified phase transition	
nominal	EDS <sup>a</sup>	Ternary eutectic reaction temperature (°C) <sup>a</sup>	Coexisting phases	Ternary transition reaction temperature (°C) <sup>a</sup>	Coexisting phases	Liquidus temperature (°C) <sup>a</sup>	Coexisting phases
Vertical section Bi-GeZn							
Bi <sub>10</sub> Ge <sub>45</sub> Zn <sub>45</sub>	Bi <sub>10.13</sub> Ge <sub>45.52</sub> Zn <sub>44.35</sub>	259.3	L'', (Ge), (Zn), (Bi)	375.8	L', L'', (Ge), (Zn)	727.3	L, (Ge)
Bi <sub>30</sub> Ge <sub>35</sub> Zn <sub>35</sub>	Bi <sub>29.11</sub> Ge <sub>35.87</sub> Zn <sub>35.02</sub>	261.8	L'', (Ge), (Zn), (Bi)	378.3	L', L'', (Ge), (Zn)	762.9	L, (Ge)
Bi <sub>60</sub> Ge <sub>20</sub> Zn <sub>20</sub>	Bi <sub>60.87</sub> Ge <sub>20.92</sub> Zn <sub>18.21</sub>	260.1	L'', (Ge), (Zn), (Bi)	-	-	728.6	L, (Ge)
Bi <sub>90</sub> Ge <sub>5</sub> Zn <sub>5</sub>	Bi <sub>89.92</sub> Ge <sub>5.73</sub> Zn <sub>4.35</sub>	246.1	L'', (Ge), (Zn), (Bi)	-	-	609.7	L, (Ge)
Vertical section Ge-BiZn							
Bi <sub>40</sub> Ge <sub>20</sub> Zn <sub>40</sub>	Bi <sub>40.18</sub> Ge <sub>19.91</sub> Zn <sub>39.91</sub>	259.4	L'', (Ge), (Zn), (Bi)	379.6	L', L'', (Ge), (Zn)	649.5	L, (Ge)
Bi <sub>30</sub> Ge <sub>40</sub> Zn <sub>30</sub>	Bi <sub>29.55</sub> Ge <sub>39.52</sub> Zn <sub>30.93</sub>	261.1	L'', (Ge), (Zn), (Bi)	381.6	L', L'', (Ge), (Zn)	788.5	L, (Ge)
Bi <sub>20</sub> Ge <sub>60</sub> Zn <sub>20</sub>	Bi <sub>20.73</sub> Ge <sub>61.01</sub> Zn <sub>18.26</sub>	255.9	L'', (Ge), (Zn), (Bi)	393.9	L', L'', (Ge), (Zn)	829.4	L, (Ge)
Bi <sub>10</sub> Ge <sub>80</sub> Zn <sub>10</sub>	Bi <sub>9.35</sub> Ge <sub>79.13</sub> Zn <sub>11.52</sub>	246.5	L'', (Ge), (Zn), (Bi)	399.6	L', L'', (Ge), (Zn)	861.6	L, (Ge)
Vertical section Zn-BiGe							
Bi <sub>45</sub> Ge <sub>45</sub> Zn <sub>10</sub>	Bi <sub>44.13</sub> Ge <sub>44.92</sub> Zn <sub>10.95</sub>	260.9	L'', (Ge), (Zn), (Bi)	328.3 (monovariant transition)	L', (Ge), (Zn)	821.6	L, (Ge)
Bi <sub>35</sub> Ge <sub>35</sub> Zn <sub>30</sub>	Bi <sub>35.82</sub> Ge <sub>34.71</sub> Zn <sub>29.47</sub>	261.9	L'', (Ge), (Zn), (Bi)	-	-	783.1	L, (Ge)
Bi <sub>25</sub> Ge <sub>25</sub> Zn <sub>50</sub>	Bi <sub>24.15</sub> Ge <sub>25.08</sub> Zn <sub>50.77</sub>	246.6	L'', (Ge), (Zn), (Bi)	-	-	679.4	L, (Ge)
Bi <sub>15</sub> Ge <sub>15</sub> Zn <sub>70</sub>	Bi <sub>15.91</sub> Ge <sub>15.19</sub> Zn <sub>68.90</sub>	250.6	L'', (Ge), (Zn), (Bi)	-	-	536.7	L, (Ge)

<sup>a</sup>Standard uncertainty (u) (0.68 level of confidence) calculated from repeated DTA measurements: for invariant reactions:  $u(T)=1.5$  °C; for monovariant phase transition:  $u(T)=2.9$  °C; for liquidus temperatures:  $u(T)=4.6$  °C;  $u(p)=1$  kPa;  $u(x)=0.1$  at. %

Table 8. Combined results of SEM-EDS and XRD analyzes of the selected Bi-Ge-Zn alloys annealed at  $T=100$  °C (standard uncertainty (u):  $u(T)=1.0$  °C) at pressure  $p=0.1$  MPa

(standard uncertainty (u):  $u(p)=1$  kPa).

N.	Composition of samples (at. %) <sup>a</sup>	Determined phases		Compositions of phases (at. %) <sup>b</sup>			Lattice parameters (Å) <sup>b</sup>	
		SEM-EDS	XRD	Bi	Ge	Zn	$a=b$	$c$
1	17.11 Bi	(Bi)	(Bi)	99.12±0.3	0.06±0.4	0.82±0.2	4.5534±0.0003	11.8251±0.0002
	42.9 Ge	(Ge)	(Ge)	0.92±0.2	98.24±0.2	0.84±0.7	5.6553±0.0003	
	39.99 Zn	(Zn)	(Zn)	0.53±0.6	0.02±0.5	99.45±0.6	2.6637±0.0001	4.9476±0.0006
2	23.02 Bi	(Bi)	(Bi)	99.15±0.5	0.30±0.3	0.55±0.4	4.5535±0.0006	11.8254±0.0006
	59.97 Ge	(Ge)	(Ge)	0.32±0.3	99.16±0.1	0.52±0.3	5.6566±0.0003	
	17.01 Zn	(Zn)	(Zn)	0.65±0.5	0.64±0.5	98.71±0.3	2.6619±0.0007	4.9446±0.0001
3	29.99 Bi	(Bi)	(Bi)	98.99±0.2	0.45±0.2	0.56±0.3	4.5523±0.0004	11.8242±0.0006
	15.94 Ge	(Ge)	(Ge)	0.32±0.5	99.26±0.5	0.42±0.4	5.6573±0.0006	
	54.07 Zn	(Zn)	(Zn)	0.56±0.1	0.14±0.6	99.30±0.1	2.6631±0.0001	4.9465±0.0005
4	61.01 Bi	(Bi)	(Bi)	99.55±0.3	0.15±0.6	0.30±0.2	4.5545±0.0002	11.8255±0.0004
	16.94 Ge	(Ge)	(Ge)	0.59±0.3	98.94±0.2	0.47±0.1	5.6561±0.0006	
	22.05 Zn	(Zn)	(Zn)	0.36±0.5	0.11±0.3	99.53±0.5	2.6641±0.0004	4.9483±0.0006
5	15.08 Bi	(Bi)	(Bi)	98.97±0.2	0.55±0.5	0.48±0.7	4.5521±0.0003	11.8236±0.0003
	4.76 Ge	(Ge)	(Ge)	0.34±0.3	98.94±0.1	0.72±0.5	5.6561±0.0001	
	80.16 Zn	(Zn)	(Zn)	0.74±0.5	0.40±0.3	98.86±0.4	2.6621±0.0006	4.9454±0.0001

<sup>a</sup>Standard uncertainty  $u(x)=0.1$  at. % (0.68 level of confidence).<sup>b</sup>Uncertainties reported inside the table are standard uncertainties, (0.68 level of confidence).

Table 9. Combined results of SEM-EDS and XRD analyzes of the selected Bi-Ge-Zn alloys annealed at  $T=300$  °C (standard uncertainty (u):  $u(T)=1.0$  °C) at pressure  $p=0.1$  MPa (standard uncertainty (u):  $u(p)=1$  kPa).

N.	Composition of samples (at. %) <sup>a</sup>	Determined phases		Compositions of phases (at. %) <sup>b</sup>			Lattice parameters (Å) <sup>b</sup>	
		SEM-EDS	XRD	Bi	Ge	Zn	$a=b$	$c$
1	15.11 Bi	L		87.39±0.5	0.20±0.3	12.41±0.8		
	54.86 Ge	(Ge)	(Ge)	0.12±0.2	99.46±0.1	0.42±0.3	5.6533±0.0001	
	30.03 Zn	(Zn)	(Zn)	0.81±0.4	0.74±0.6	98.45±0.3	2.6612±0.0003	4.9437±0.0005
2	30.02 Bi	L		87.55±0.6	0.10±0.3	12.35±0.2		
	9.97 Ge	(Ge)	(Ge)	0.22±0.2	99.38±0.1	0.40±0.2	5.6527±0.0007	
	60.01 Zn	(Zn)	(Zn)	0.71±0.6	0.17±0.6	99.12±0.5	2.6629±0.0002	4.9446±0.0006
3	45.10 Bi	L		86.29±0.2	0.65±0.1	13.06±0.3		
	14.83 Ge	(Ge)	(Ge)	0.21±0.4	99.40±0.5	0.39±0.4	5.6529±0.0005	
	40.07 Zn	(Zn)	(Zn)	0.56±0.1	0.14±0.6	99.30±0.5	2.6636±0.0004	4.9465±0.0001
4	61.01 Bi	L		90.65±0.3	0.15±0.6	9.20±0.2		
	38.68 Ge	(Ge)	(Ge)	0.59±0.3	99.04±0.2	0.37±0.1	5.6522±0.0007	
	0.31 Zn							
5	82.08 Bi	L		93.97±0.1	0.55±0.4	5.48±0.8		
	17.21 Ge	(Ge)	(Ge)	0.34±0.2	98.94±0.2	0.72±0.4	5.6516±0.0002	
	0.71 Zn							

<sup>a</sup>Standard uncertainty  $u(x)=0.1$  at. % (0.68 level of confidence).<sup>b</sup>Uncertainties reported inside the table are standard uncertainties, (0.68 level of confidence).

Table 10. Predicted invariant reaction of the ternary Bi-Ge-Zn system.

T (°C)	Reaction	Type	Composition (mol)		
			x(Bi)	x(Ge)	x(Zn)
389.19	$L \rightarrow L+(Zn)+(Ge)$	E1	0.6678	0.0125	0.3197
254.44	$L \rightarrow (Zn)+(Ge)+(Bi)$	E2	0.9186	0.0003	0.0811

Journal Pre-proofs

## Highlights

- ▶ Experimental investigation of the phase transformations temperatures.
- ▶ Experimental investigation of phase equilibria at 100 °C and 300 °C.
- ▶ Thermodynamic optimization of Bi-Ge-Zn liquid phase.
- ▶ Calculated liquidus surface projection and determined invariant reaction.
- ▶ Good agreement of calculation and experimental data is reached.